Dyes and Pigments 136 (2017) 168–174

Contents lists available at ScienceDirect

Dyes and Pigments

journal homepage: www.elsevier.com/locate/dyepig

Dithienopyrrole compound with twisted triphenylamine termini: Reversible near-infrared electrochromic and mechanochromic dual-responsive characteristics

Jing Zhang [a, 1], Zhao Chen [a, 1], Lan Yang [a], Fang Hu [b], Guang-Ao Yu [a], Jun Yin [a, **], Sheng-Hua Liu [a, *]

[a] Key Laboratory of Pesticide and Chemical Biology, Ministry of Education, College of Chemistry, Central China Normal University, Wuhan 430079, PR China
[b] School of Materials Science and Chemical Engineering, Ningbo University, Ningbo 315211, PR China

ARTICLE INFO

Article history:
Received 20 June 2016
Received in revised form
4 August 2016
Accepted 22 August 2016
Available online 24 August 2016

Keywords:
Dithieno[3,2-*b*:2′,3′-*d*]pyrrole
Triphenylamine
Mechanochromic properties
Electrochromic properties
Fluorescence
Density functional theory

ABSTRACT

A dithieno[3,2-*b*:2′,3′-*d*]pyrrole-based luminogen **1** has been synthesized by appending two twisted triphenylamine units to the rigid conjugated dithieno[3,2-*b*:2′,3′-*d*]pyrrole core. This compound exhibits reversible mechanochromic luminescence in the solid state and near-infrared electrochromic switching behavior in solution. A reversible switching in fluorescence color between yellow-green and green can be observed through mechanical grinding and vapor fuming of solid powdered **1**, which involves an interconversion between a crystalline form and an amorphous phase according to X-ray diffraction analysis. The associated oxidized species of **1** show intense redox-switchable near-infrared absorption and different fluorescence colors in solution in spectroelectrochemical and luminescence measurements. Density functional theory calculations have confirmed that there is considerable electron delocalization between the dithieno[3,2-*b*:2′,3′-*d*]pyrrole linker and two triphenylamine redox-active termini during the oxidation process.

1. Introduction

The study of systems that exhibit facile bridge-mediated electron transfer between organic, organometallic, and inorganic termini has received considerable recent attention due to their application prospects in building highly functionalized molecular electronic devices [1–10]. Specifically, compounds with two redox-active groups linked by a rigid π-conjugated bridge are considered among the most promising systems serving as molecular wires because of their easy functionalization, tunability, and the low cost of the requisite molecules [11–16]. More interestingly, these systems usually show strong changes in their electronic spectra in the near-infrared (NIR) region and different colors associated with their different oxidation states. Accordingly, the above NIR electrochromic phenomenon, as an intelligent response to an external stimulus, might be applied to the control of both light transmission (windows) and reflection (mirrors), and used in diverse switchable display devices, biological sensing, data storage, and so on [17–20]. Meanwhile, the mechanochromic phenomenon, as another interesting kind of intelligent response, has also been extensively studied in recent years [21,22]. In particular, mechanochromic luminescent materials that change their solid-state fluorescence characteristics upon mechanical stimulus have many potential applications in the fields of sensors, security inks, and memory devices. To date, a number of organic and metal-bearing mechanofluorochromic materials have been found [23–32].

Because of their fused, rigid backbone and good molecular planarity, dithieno[3,2-*b*:2′,3′-*d*]pyrrole (DTP) structural motifs have sparked immense interest concerning their applications in a variety of materials [33]. It has been well documented that the introduction of DTP units imparts enhanced conjugation, high conductivity, and high charge carrier mobility to electronic materials, such as organic light-emitting diodes (OLEDs) [34], organic photovoltaic devices (OPVs) [35,36], and organic field-effect transistors (OFETs) [37], as well as enhanced solution and solid-state fluorescence to organic materials [38]. Meanwhile, the propeller-

* Corresponding author.
** Corresponding author.
E-mail addresses: yinj@mail.ccnu.edu.cn (J. Yin), chshliu@mail.ccnu.edu.cn (S.-H. Liu).
[1] These authors contributed equally to this work.

http://dx.doi.org/10.1016/j.dyepig.2016.08.051
0143-7208/

shaped triphenylamine (TPA) moiety has been widely used for the construction of diverse optoelectronic materials, due to its strong electron-donating ability, good hole-transporting capability, and high light-to-electrical energy conversion efficiency [39,40]. In addition, TPA-based derivatives with twisted molecular conformation have recently been reported to display stimuli-responsive solid-state fluorescence switching behavior [41,42]. The intriguing possibility of integrating the DTP unit with electro-active triphenylamine termini with a unique twisted molecular conformation attracted our interest. The resulting system was expected to exhibit integrated dual- or even multifunctional intelligent responses to external stimuli, including at least electric and mechanical forces. In this work, a DTP derivative (**1**, Chart 1) bearing two triphenylamine termini has been synthesized by Suzuki coupling of dibromo-substituted dithienopyrrole and triphenylamine boronic acid. The two-factor electrochromic and mechanochromic responsive behaviors of **1** have been systematically investigated by means of photoluminescence spectroscopy, electrochemistry, and spectroelectrochemistry, supplemented by DFT calculations.

2. Materials and methods

2.1. General materials and synthesis

All manipulations were carried out under a dry argon atmosphere using standard Schlenk techniques, unless stated otherwise. Solvents were pre-dried and distilled under argon prior to use, except those used directly for spectroscopic measurements, which were of spectroscopic grade. The starting material 2,6-dibromo-4-butyl-4*H*-dithieno[3,2-*b*:2′,3′-*d*]pyrrole was prepared according to procedures described in the literature [43]. Other reagents were purchased and used as received.

2,6-Dibromo-4-butyl-4*H*-dithieno[3,2-*b*:2′,3′-*d*]pyrrole (235 mg, 0.60 mmol) and (4-(diphenylamino)phenyl)boronic acid (532 mg, 1.38 mmol) were dissolved in toluene (15 mL) under N_2. 2 M aqueous K_2CO_3 solution (4 mL) was added, N_2 was bubbled through the mixture for 30 min, and then $Pd(PPh_3)_4$ (23 mg, 0.02 mmol) was added. After stirring overnight at 110 °C, the reaction mixture was cooled to room temperature and extracted with CH_2Cl_2. The combined organic layers were dried over Na_2SO_4. The solvent was removed in vacuo, and the residue was purified by chromatography on silica gel (petroleum ether/CH_2Cl_2, 8:1). The product was precipitated from a solution in CH_2Cl_2 by the addition of MeOH to give 388 mg (78%) of a yellow powder. ^{1}H NMR (C_6D_6, 400 MHz, ppm): δ = 0.71 (t, *J* = 8 Hz, 3H), 1.08 (m, 2H), 1.50 (m, 2H), 3.67 (s, 2H), 6.88 (m, 2H), 7.02–7.12 (m, 22H), 7.47 (d, *J* = 8 Hz, 4H); ^{13}C NMR (C_6D_6, 100 MHz, ppm): δ = 14.5, 21.0, 31.2, 47.4, 106.9, 115.2, 123.6, 125.0, 125.1, 127.0, 130.0, 130.9, 142.5, 145.8, 147.6, 148.4; elemental analysis calcd. (%) for $C_{48}H_{39}N_3S_2$: C 79.85, H 5.44, N 5.82; found: C 79.59, H 5.22, N 5.78.

2.2. Physical measurements

^{1}H and ^{13}C NMR spectra were collected on a Varian Mercury Plus 400 spectrometer (400 MHz). ^{1}H and ^{13}C NMR chemical shifts are relative to TMS. Elemental analyses (C, H, N) were performed with a Vario El III CHNSO instrument. Electrochemical measurements were performed on a CHI 660C potentiostat (CHI, Austin, TX, USA). A three-electrode single-compartment cell was used for the solution of complex and supporting electrolyte in dry CH_2Cl_2. The solution was deaerated by argon bubbling on a frit for about 10 min before the measurement. The analyte and electrolyte (*n*-Bu_4NPF_6) concentrations were typically 10^{-3} and 10^{-1} mol dm^{-3}, respectively. A 500-μm diameter platinum disk working electrode, a platinum wire counter electrode, and an Ag/Ag^+ reference electrode were used. Spectroelectrochemical experiments at room temperature were performed with an airtight optically transparent thin-layer electrochemical (OTTLE) cell (optical path length of ca. 200 μm) equipped with a Pt minigrid working electrode and CaF_2 windows [44]. The cell was positioned in the sample compartment of a Shimadzu UV-3600 UV-vis-NIR spectrophotometer. Controlled-potential electrolyses were carried out with a CHI 660C potentiostat. The sample concentrations were ca. 2×10^{-3} mol dm^{-3}, and 10^{-1} M *n*-Bu_4NPF_6 was used as the supporting electrolyte. Compound **1** was oxidized in a stepwise manner, increasing the anodic potential in steps of 10 or 20 mV. Fluorescence spectra were recorded on a Hitachi F-4500 fluorescence spectrophotometer or a Fluoromax-P luminescence spectrometer (Horiba–Jobin-Yvon Inc., Edison, NJ, USA). XRD studies were conducted on a Shimadzu XRD-6000 diffractometer using Ni-filtered and graphite-monochromated Cu-K_α radiation (λ = 1.54 Å, 40 kV, 30 mA).

2.3. X-ray crystallography

Intensity data were collected on a Nonius Kappa CCD diffractometer with Mo-K_α radiation (0.71073 Å) at room temperature. The structures were solved by a combination of direct methods (SHELXS-97) [45] and Fourier difference techniques and refined by full-matrix least-squares techniques (SHELXL-97) [46]. All non-H atoms were refined anisotropically. Crystallographic data for the structure in this paper have been deposited with the Cambridge Crystallographic Data Centre as supplementary publication CCDC-1478249.

2.4. Computational details

DFT calculations were performed with the Gaussian 09 program [47] at the B3LYP/6-31G* level of theory. Geometry optimizations were performed without any symmetry constraints, and frequency calculations on the resulting optimized geometries showed no imaginary frequencies. Electronic transitions were calculated by the time-dependent DFT (TD-DFT) method. The MO contributions were generated using the Multiwfn2.6.1_bin_Win package and plotted using GaussView 5.0. Solvation effects in dichloromethane are included in some of the calculations by applying the conductor-like polarizable continuum model (CPCM) [48,49].

3. Results and discussion

3.1. Synthesis and characterization

The 2,6-dibromo-4-butyl-4*H*-dithieno[3,2-*b*:2′,3′-*d*]pyrrole precursor was synthesized by the method reported in the literature [43]. The target compound **1** was prepared in good yield through a Pd-catalyzed Suzuki coupling reaction between the 2,6-dibromo-dithieno[3,2-*b*:2′,3′-*d*]pyrrole precursor and 4-(diphenylamino) phenyl)boronic acid, as shown in Scheme 1 (for details, see the Experimental Section).

3.2. Mechanofluorochromic behavior

The mechanochromic luminescence behavior of **1** was investigated by photoluminescence (PL) spectroscopy. As shown in Fig. 1, the PL spectrum of the initial solid **1** showed two emission bands with maxima (λ_{max}) at 516 and 550 nm, respectively. Correspondingly, yellow-green fluorescence was observed under UV light at a wavelength of 365 nm. However, upon grinding the solid powdered **1** with a pestle in a mortar, a broad emission band with λ_{max} = 518 nm, as well as an obvious change in emission color from

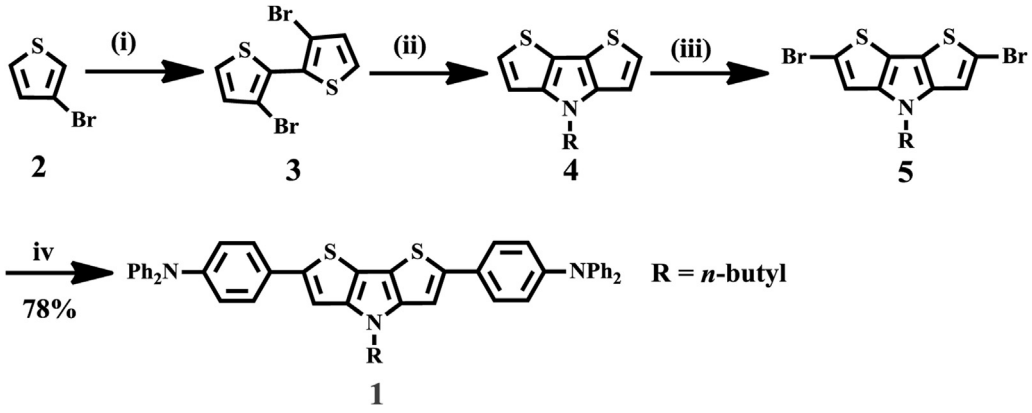

Scheme 1. General synthetic routes to compound **1**. Reagents and conditions: (i) LDA (lithium diisopropylamide), $CuCl_2$, THF, at 0 °C; (ii) [$Pa_2(dba)_3$] (tris(dibenzylideneacetone) dipalladium(0)), dppf (1, 1′-bis(diphenyl-phosphino)ferrocene), *n*-butylamine, in toluene, reflux for 24 h; (iii) NBS, in DMF, at 0 °C; (iv) (4-(diphenylamino)phenyl)boronic acid, $Pd(PPh_3)_4$, K_2CO_3, in toluene/H_2O, reflux for 24 h.

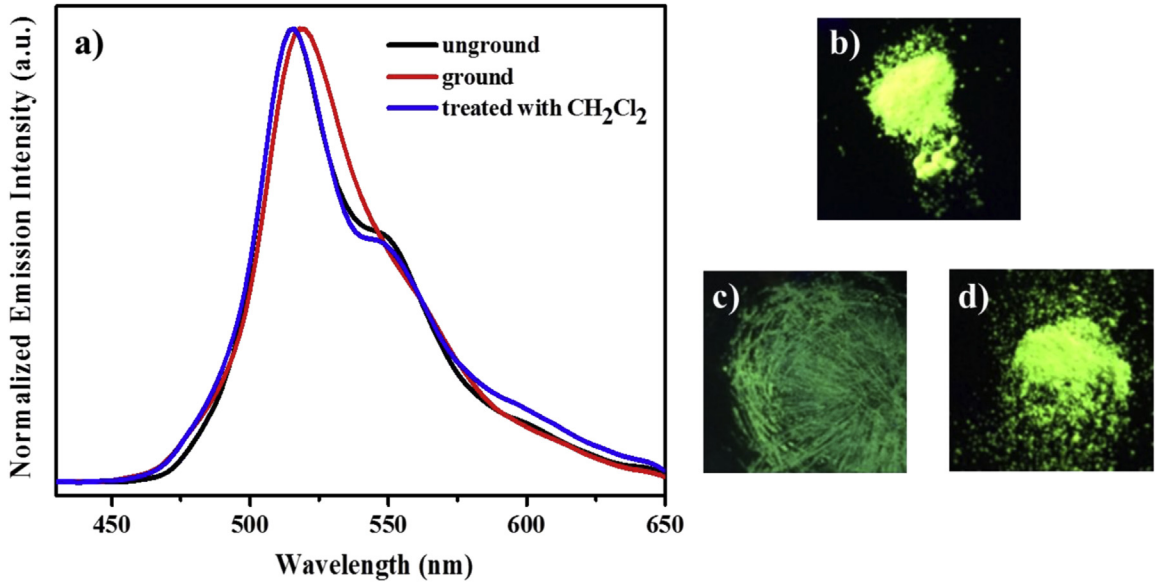

Fig. 1. (a) PL spectra of compound **1** before grinding, after grinding, and after treatment with dichloromethane vapor. Excitation wavelength: 365 nm. Fluorescence images of **1** under irradiation with 365 nm UV light: (b) the initial solid sample; (c) the ground solid sample; (d) the dichloromethane-fumed ground solid sample.

yellow-green to green, was clearly observed. This interesting phenomenon indicated that compound **1** exhibited luminescence mechanochromic behavior. Furthermore, the bright yellow-green fluorescence was recovered when the ground solid sample was fumed with dichloromethane vapor for 1 min. Therefore, the mechanochromic luminescence behavior of compound **1** was also reversible. It is well known that the mechanochromic property can usually be attributed to a variation in molecular morphology [50–53]. Thus, in order to probe this possible mechanochromic mechanism in compound **1**, powder X-ray diffraction (XRD) measurements were carried out. As shown in Fig. 2, the XRD pattern of the initial solid sample **1** exhibited a number of clear and intense peaks, consistent with its crystalline nature. After grinding, however, these intense reflection peaks could no longer be observed, indicating that an amorphous phase had been generated. Following fuming treatment of the ground sample with dichloromethane vapor, the initial intense peaks were restored, which implied that this treatment resulted in an amorphous to crystalline phase conversion. Hence, the powder XRD results confirmed that a reversible conversion between a crystalline state and an amorphous state is responsible for the interesting mechanochromic luminescence behavior of compound **1**.

3.3. X-ray crystal structure

Fortunately, crystals of compound **1** suitable for X-ray structure analysis could be obtained by recrystallization from dichloromethane/methanol. Detailed crystal data can be found in Table S1 (ESI†). The corresponding bond angles and distances are provided in Table S2 (ESI†). As can be seen from the structural organization of compound **1** (Fig. 3), weak intermolecular C-H$\cdots\pi$ interactions (d = 2.700 Å, 2.524 Å, Fig. 3) facilitate the molecular packing. However, the twisted molecular conformation and the absence of a strong intermolecular force lead to a loose packing motif of compound **1** [54,55]. Thus, the ordered crystal packing may readily collapse upon exposure to external pressure. As a result, the fluorescence color of compound **1** changed from yellow-green to green.

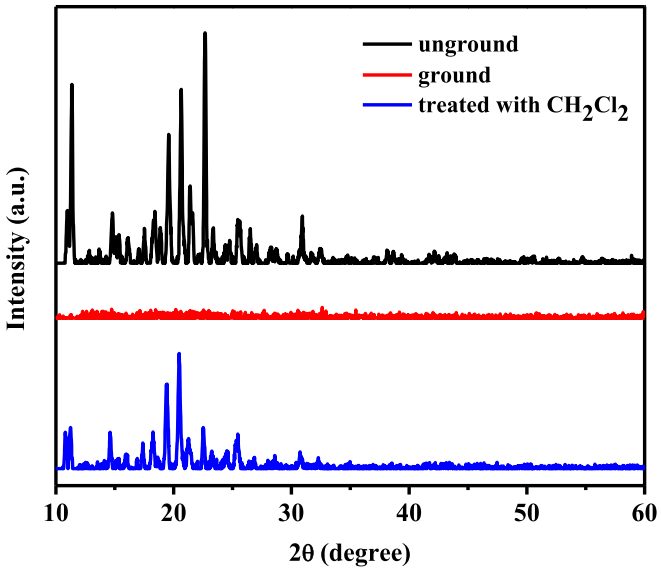

Fig. 2. XRD patterns of compound **1**: unground, ground and after treatment with dichloromethane vapor.

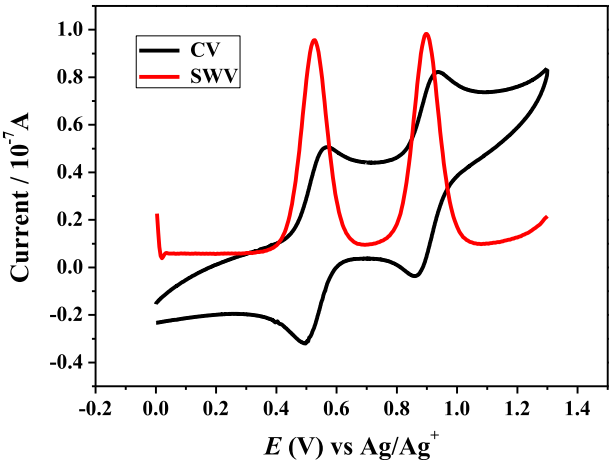

Fig. 4. Cyclic voltammogram (black line, CH_2Cl_2/0.1 M n-Bu_4NPF_6, 298 K at 0.1 V s^{-1}) and square-wave voltammogram (red line, f = 10 Hz) of compound **1**. (For interpretation of the references to colour in this figure legend, the reader is referred to the web version of this article.)

3.4. Electrochemical behavior

Subsequently, in order to explore the electronic properties of compound **1**, we carried out electrochemical measurements (cyclic voltammograms and square-wave voltammograms) [56,57]. As shown in Fig. 4, compound **1** exhibited two consecutive reversible redox processes at 0.08 V and 0.47 V vs. ferrocene/ferrocenium (Fc/Fc^+). These can be ascribed to oxidations centered on the amine terminal and thienopyrrole bridge, respectively, based on comparison with the anodic potentials of the dibromo precursor (0.60 V vs. Fc/Fc^+) and triphenylamine (0.49 V vs. Fc/Fc^+) (Fig. S1). The first step of the two-electron oxidation process involved both TPA termini to equal extents. Therefore, we carried out calculations on the monocationic state in the following section for brevity. According to DFT calculations on $\mathbf{1}^+$, the relatively low potential of the amine-based oxidation in compound **1** may possibly be attributed to the considerable electron delocalization throughout the whole molecular framework (*vide infra*) [58,59].

3.5. Spectroscopic investigations on the oxidized forms

To gain further insight into the electron-transfer process, *in situ* spectroelectrochemical studies were carried out by increasing the anodic potential in steps of 10 or 20 mV in an optically transparent thin-layer electrochemical (OTTLE) cell. As presented in Fig. 5, during the first two-electron oxidation process, several new absorption bands appeared at around 600 nm and continually increased, and strong absorptions in the near-IR region (800–2000 nm) appeared simultaneously. According to the prediction of TD-DFT calculations (Fig. 6), the lower-energy absorptions in the NIR region are mainly associated with β-HOSO→β-LUSO and α-HOSO→α-LUSO excitations, being attributed to inter-ligand charge-transfer (CT) transitions with some admixed ligand (TPA)→N^+ component. The lower-energy transitions in the visible region (around 600 nm) can be primarily assigned to α-HOSO→α-LUSO and β-HOSO-3→β-LUSO transitions with prominent intra-

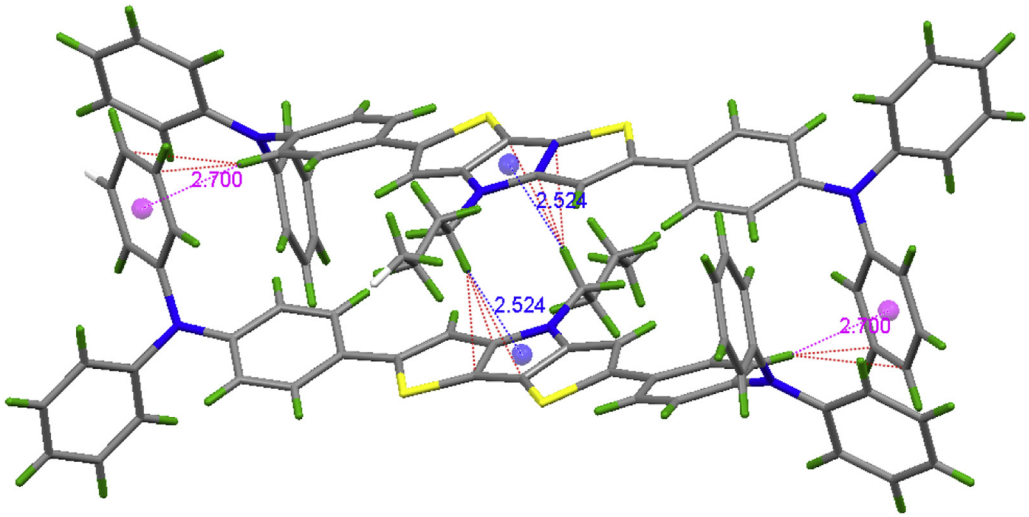

Fig. 3. The structural organization of compound **1**.

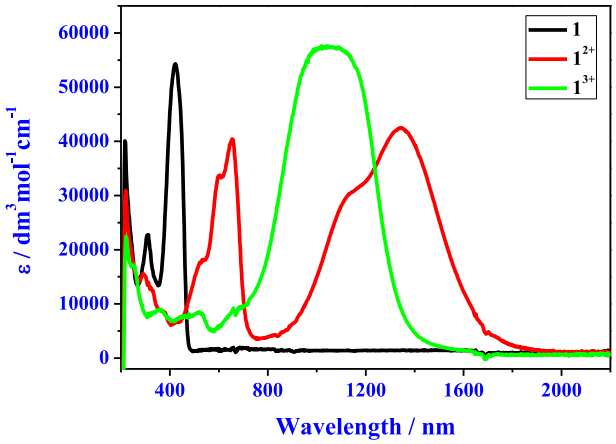

Fig. 5. UV-Vis-NIR absorption spectra of **1** (black), $\mathbf{1}^{2+}$ (red) and $\mathbf{1}^{3+}$ (green) in CH_2Cl_2/0.1 M *n*-Bu_4NPF_6 at 298 K within an optically transparent thin-layer electrochemical (OTTLE) cell. (For interpretation of the references to colour in this figure legend, the reader is referred to the web version of this article.)

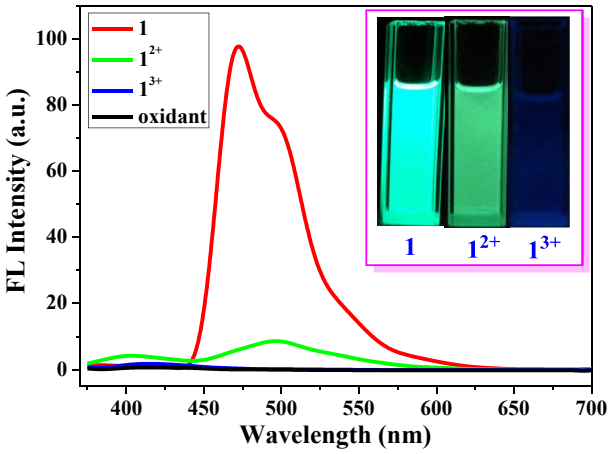

Fig. 7. PL spectra of luminogen **1** (red), $\mathbf{1}^{2+}$ (green), and $\mathbf{1}^{3+}$ (blue) recorded in the course of stepwise oxidation of **1** by adding 0, 2 and 3 equivalent of oxidant $[N(C_6H_4\text{-}Br\text{-}4)_3]^+[SbCl_6]^-$ in CH_2Cl_2 at room temperature (1.0×10^{-5} mol L^{-1}). Excitation wavelength = 365 nm. Inset: fluorescence images of **1**, $\mathbf{1}^{2+}$, and $\mathbf{1}^{3+}$ under 365 nm UV light (1.0×10^{-5} mol L^{-1}). (For interpretation of the references to colour in this figure legend, the reader is referred to the web version of this article.)

ligand CT, inter-ligand CT, and appropriate $N \rightarrow N^+$ character. The above observations confirmed remarkable delocalization throughout the DTP and TPA units, and that the contribution from the DTP core is significant during the oxidation process. Following further oxidation to $\mathbf{1}^{3+}$, all of the absorption features associated with the TPA framework disappeared, and a new band appeared at

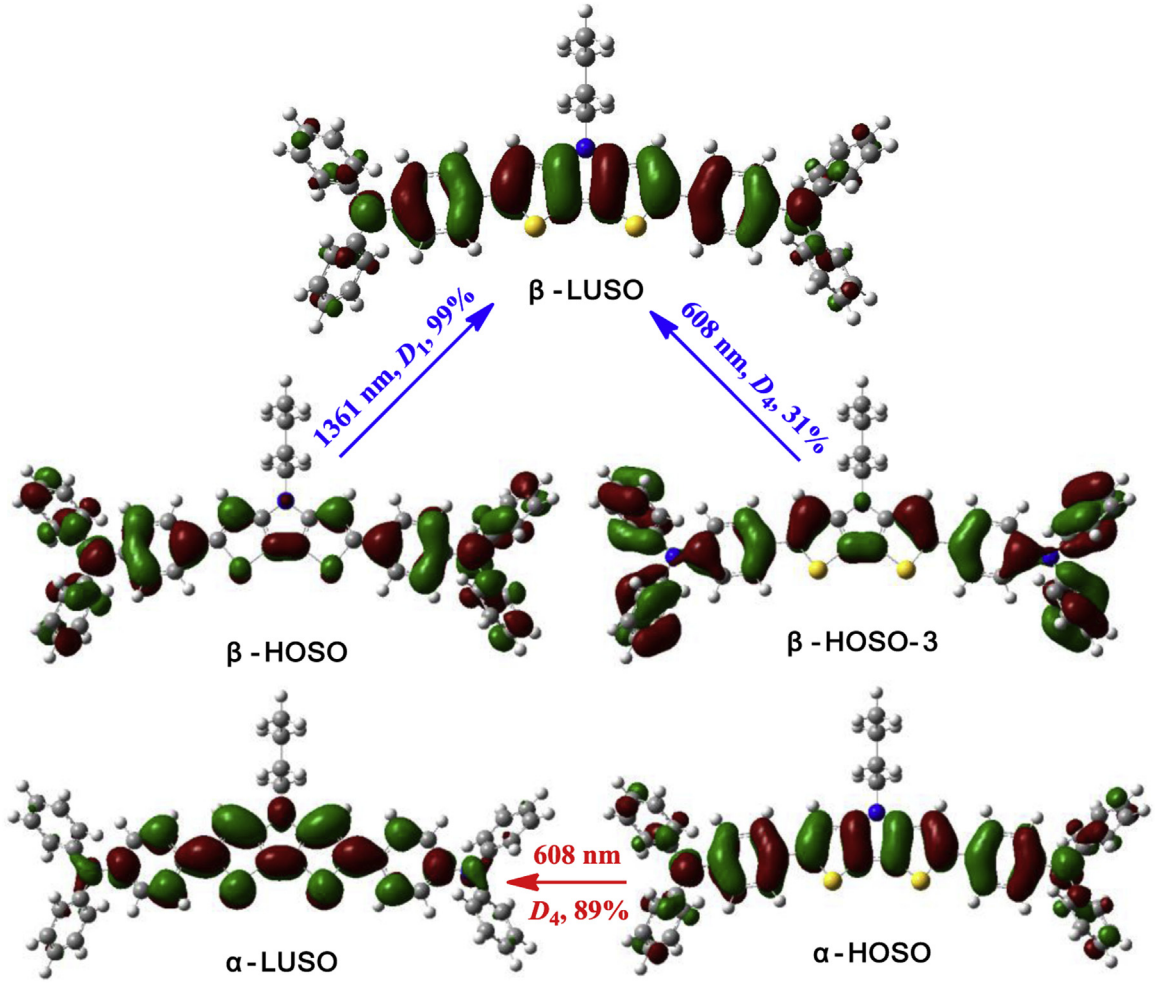

Fig. 6. Spin orbitals involved in the major electronic excitations in $\mathbf{1}^+$ (D = doublet). B3LYP/6-31G*/CPCM/CH_2Cl_2.

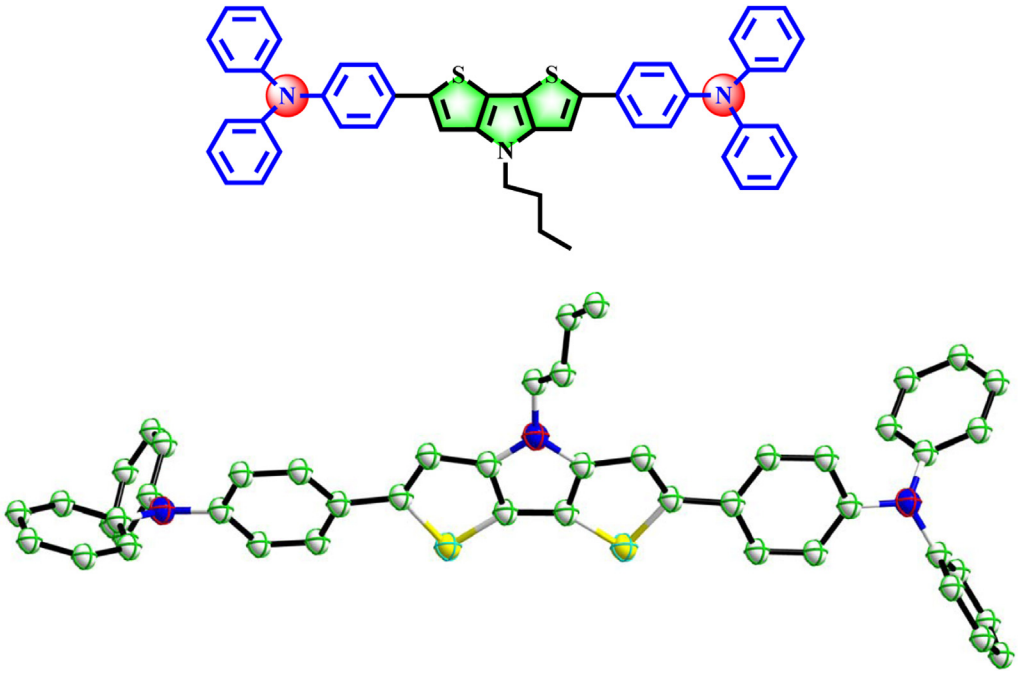

Chart 1. The molecular structure (top) and single crystal structure (bottom) of compound **1**.

around 1050 nm due to localized oxidation of the DTP core. The above spectral changes upon stepwise oxidation and reduction proved to be essentially reversible (Fig. 5). More intriguingly, compound **1** exhibited different emission behaviors in different oxidation states in solution, as shown in Fig. 6, and different associated fluorescence colors under UV light at a wavelength of 365 nm (Fig. 7). The above observations indicate that this compound may potentially be used as an electroswitchable electrochromic material.

4. Conclusions

A DTP derivative with two twisted TPA termini has been developed. It exhibits two consecutive oxidation steps at relatively low anodic potentials as a result of a high level of electron delocalization between the TPA groups. The rigid DTP linking core makes a significant contribution to the oxidation process, based on the results of electrochemistry, spectroelectrochemistry, and DFT calculations. UV/Vis/NIR spectroelectrochemical studies have indicated that the associated oxidized species of compound **1** show strong redox-switchable NIR absorptions in solution, accompanied by an obvious change in luminescence color. Mechanofluorochromic studies have shown that mechanical grinding of powdered **1** leads to an obvious change in its fluorescence color from yellow-green to green, as a result of the collapse of weak intermolecular C-H$\cdots\pi$ interactions. XRD analysis has revealed that the observed reversible fluorescence switching is associated with an interconversion between a crystalline state and an amorphous phase. Dichloromethane vapor fuming of the amorphous phase leads to reversion to the crystalline phase. Therefore, our studies have indicated that this compound might serve as a promising electrochromic and mechanochromic switching material. More importantly, this work may be helpful for the exploration of new intelligent materials displaying multifunctional responsive behaviors.

Acknowledgements

The authors acknowledge financial support from National Natural Science Foundation of China (21272088, 21472059, 21402057), the self-determined research funds of CCNU from the colleges' basic research and operation of MOE (CCNU14A05009, CCNU14F01003) and the excellent doctorial dissertation cultivation grant from Central China Normal University (2015YBYB108, 2015YBZD004).

Appendix A. Supplementary data

Supplementary data related to this article can be found at http://dx.doi.org/10.1016/j.dyepig.2016.08.051.

References

[1] Fox MA, Roberts RL, Baines TE, Le Guennic B, Halet JF, Hartl F, et al. Ruthenium complexes of C, C'-bis (ethynyl) carboranes: an investigation of electronic interactions mediated by spherical pseudo-aromatic spacers. J Am Chem Soc 2008;130:3566–78.
[2] Brunschwig BS, Creutz C, Sutin N. Electroabsorption spectroscopy of charge transfer states of transition metal complexes. Coord Chem Rev 1998;177:61–79.
[3] Carroll RL, Gorman CB. The genesis of molecular electronics. Angew Chem Int Ed 2002;41:4378–400.
[4] Paul F, Lapinte C. Organometallic molecular wires and other nanoscale-sized devices: an approach using the organoiron (dppe)Cp* Fe building block. Coord Chem Rev 1998;178–180:431–509.
[5] Pevny F, Di Piazza E, Norel L, Drescher M, Winter RF, Rigaut S. Fully delocalized (ethynyl)(vinyl) phenylene-bridged diruthenium radical complexes. Organometallics 2010;29:5912–8.
[6] Aguirre-Etcheverry P, O'Hare D. Electronic communication through unsaturated hydrocarbon bridges in homobimetallic organometallic complexes. Chem Rev 2010;110:4839–64.
[7] Linseis M, Záliš S, Zabel M, Winter RF. Ruthenium stilbenyl and diruthenium distyrylethene complexes: aspects of electron delocalization and electrocatalyzed isomerization of the Z-isomer. J Am Chem Soc 2012;134:16671–92.
[8] Záliš S, Winter RF, Kaim W. Quantum chemical interpretation of redox properties of ruthenium complexes with vinyl and TCNX type non-innocent ligands. Coord Chem Rev 2010;254:1383–96.
[9] Shi YH, Yee GT, Wang GB, Ren T. A new direction in carbon-rich

organometallic wires: diruthenium compounds bridged by *E*-Hex-3-ene-1, 5-diyn-diyl. J Am Chem Soc 2004;126:10552–3.
[10] Xu GL, Crutchley RJ, DeRosa MC, Pan QJ, Zhang HX, Wang X, et al. Strong electronic couplings between ferrocenyl centers mediated by bis-ethynyl/butadiynyl diruthenium bridges. J Am Chem Soc 2005;127:13354–63.
[11] Rigaut S, Olivier C, Costuas K, Choua S, Fadhel O, Massue J, et al. C7 and C9 carbon-rich bridges in diruthenium systems: synthesis, spectroscopic, and theoretical investigations of different oxidation states. J Am Chem Soc 2006;128:5859–76.
[12] Gao LB, Liu SH, Zhang LY, Shi LX, Chen ZN. Preparation, characterization, redox properties, and UV-vis-NIR spectra of binuclear ruthenium complexes $[\{(Phtpy)(PPh_3)_2Ru\}_2\{C{:}C\text{-}(CH{=}CH)_m\text{-}C{:}C\}]^{n+}$ (Phtpy = 4'-phenyl-2,2':6',2''-terpyridine). Organometallics 2006;25:506–12.
[13] Yao CJ, Zhong YW, Yao JN. Charge delocalization in a cyclometalated bisruthenium complex bridged by a noninnocent 1, 2, 4, 5-tetra (2-pyridyl) benzene ligand. J Am Chem Soc 2011;133:15697–706.
[14] Cui BB, Tang JH, Yao JN, Zhong YW. A molecular platform for multistate near-infrared electrochromism and flip-flop, flip-flap-flop, and ternary memory. Angew Chem Int Ed 2015;54:9192–7.
[15] Zhang J, Zhang MX, Sun CF, Xu M, Hartl F, Yin J, et al. Diruthenium complexes with bridging diethynyl polyaromatic ligands: synthesis, spectroelectrochemistry, and theoretical calculations. Organometallics 2015;34:3967–78.
[16] Zhang J, Sun CF, Zhang MX, Hartl F, Yin J, Yu GA, et al. Asymmetric oxidation of vinyl-and ethynyl terthiophene ligands in triruthenium complexes. Dalton Trans 2016;45:768–82.
[17] Mortimer RJ. Electrochromic materials. Chem Soc Rev 1997;26:147–56.
[18] Nie HJ, Shao JY, Yao CJ, Zhong YW. Organic-inorganic mixed-valence systems with strongly-coupled triarylamine and cyclometalated osmium. Chem Commun 2014;50:10082–5.
[19] Ward MD. Near-infrared electrochromic materials for optical attenuation based on transition-metal coordination complexes. J Solid State Electrochem 2005;9:778–87.
[20] Zheng J, Qiao W, Wan X, Gao JP, Wan ZY. Near-infrared electrochromic and chiroptical switching materials: design, synthesis, and characterization of chiral organogels containing stacked naphthalene diimide chromophores. Chem Mater 2008;20:6163–8.
[21] Chi Z, Zhang X, Xu B, Zhou X, Ma C, Zhang Y, et al. Recent advances in organic mechanofluorochromic materials. Chem Soc Rev 2012;41:3878–96.
[22] Sagara Y, Komatsu T, Ueno T, Hanaoka K, Kato T, Nagano T. Covalent attachment of mechanoresponsive luminescent micelles to glasses and polymers in aqueous conditions. J Am Chem Soc 2014;136:4273–80.
[23] Yoon SJ, Chung JW, Gierschner J, Kim KS, Choi MG, Kim D, et al. Multistimuli two-color luminescence switching via different slip-stacking of highly fluorescent molecular sheets. J Am Chem Soc 2010;132:13675–83.
[24] Dong Y, Xu B, Zhang J, Tan X, Wang L, Chen J, et al. Piezochromic luminescence based on the molecular aggregation of 9,10-bis((*E*)-2-(pyrid-2-yl)vinyl) anthracene. Angew Chem Int Ed 2012;51:10782–5.
[25] Han T, Zhang Y, Feng X, Lin Z, Tong B, Shi J, et al. Reversible and hydrogen bonding-assisted piezochromic luminescence for solid-state tetraaryl-buta-1, 3-diene. Chem Commun 2013;49:7049–51.
[26] Wang X, Liu Q, Yan H, Liu Z, Yao M, Zhang Q, et al. Piezochromic luminescence behaviors of two new benzothiazole–enamido boron difluoride complexes: intra-and inter-molecular effects induced by hydrostatic compression. Chem Commun 2015;51:7497–500.
[27] Chen Z, Zhang J, Song M, Yin J, Yu GA, Liu SH. A novel fluorene-based aggregation-induced emission (AIE)-active gold(I) complex with crystallization-induced emission enhancement (CIEE) and reversible mechanochromism characteristics. Chem Commun 2015;51:326–9.
[28] Chen Z, Huang PS, Li Z, Yin J, Yu GA, Liu SH. Triisocyano-based trinuclear gold(I) complexes with aggregation-induced emission (AIE) and mechanochromic luminescence characteristics. Inorganica Chim Acta 2015;432:192–7.
[29] Ito H, Saito T, Oshima N, Kitamura N, Ishizaka S, Hinatsu Y, et al. Reversible mechanochromic luminescence of $[(C_6F_5Au)_2(\mu\text{-}1,4\text{-diisocyanobenzene})]$. J Am Chem Soc 2008;130:10044–5.
[30] Xu B, Chi Z, Zhang X, Li H, Chen C, Liu S, et al. A new ligand and its complex with multi-stimuli-responsive and aggregation-induced emission effects. Chem Commun 2011;47:11080–2.
[31] Xu S, Liu T, Mu Y, Wang YF, Chi Z, Lo CC, et al. An organic molecule with asymmetric structure exhibiting aggregation-induced emission, delayed fluorescence, and mechanoluminescence. Angew Chem Int Ed 2015;54:874–8.
[32] Chen Z, Li Z, Yang L, Liang J, Yin J, Yu GA, et al. Novel diisocyano-based dinuclear gold(I) complexes with aggregation-induced emission and mechanochromism characteristics. Dyes Pigments 2015;121:170–7.
[33] Ogawa K, Rasmussen SC. A simple and efficient route to N-functionalized dithieno [3, 2-*b*: 2', 3'-*d*] pyrroles: fused-ring building blocks for new conjugated polymeric systems. J Org Chem 2003;68:2921–8.
[34] Zhang H, Fan J, Iqbal Z, Kuang DB, Wanga L, Meier H, et al. Novel dithieno [3, 2-*b*: 2′, 3′-*d*] pyrrole-based organic dyes with high molar extinction coefficient for dye-sensitized solar cells. Org Electron 2013;14:2071–81.
[35] Zhou E, Nakamura M, Nishizawa T, Zhang Y, Wei Q, Tajima K, et al. Synthesis and photovoltaic properties of a novel low band gap polymer based on N-substituted dithieno [3, 2-*b*: 2′, 3′-*d*] pyrrole. Macromolecules 2008;41:8302–5.
[36] Zhou E, Yamakawa S, Tajima K, Yang C, Hashimoto K. Synthesis and photovoltaic properties of diketopyrrolopyrrole-based donor-acceptor copolymers. Chem Mater 2009;21:4055–61.
[37] Liu J, Zhang R, SauvéG Kowalewski T, McCullough RD. Highly disordered polymer field effect transistors: N-alkyl dithieno [3, 2-*b*: 2′, 3′-*d*] pyrrole-based copolymers with surprisingly high charge carrier mobilities. J Am Chem Soc 2008;130:13167–76.
[38] Rasmussen SC, Evenson SJ. Dithieno [3, 2-*b*: 2′, 3′-*d*] pyrrole-based materials: synthesis and application to organic electronics. Prog Polym Sci 2013;38:1773–804.
[39] Thomas KJ, Hsu YC, Lin JT, Lee KM, Ho KC, Lai CH, et al. 2, 3-Disubstituted thiophene-based organic dyes for solar cells. Chem Mater 2008;20:1830–40.
[40] Tian H, Yang X, Pan J, Chen R, Liu M, Zhang Q, et al. A triphenylamine dye model for the study of intramolecular energy transfer and charge transfer in dye-sensitized solar cells. Adv Funct Mater 2008;18:3461–8.
[41] Kwon MS, Gierschner J, Yoon SJ, Park SY. Unique piezochromic fluorescence behavior of dicyanodistyrylbenzene based donor-acceptor-donor triad: mechanically controlled photo-induced electron transfer (eT) in molecular assemblies. Adv Mater 2012;24:5487–92.
[42] Chan CYK, Lam JWY, Zhao Z, Chen S, Lu P, Sung HHY, et al. Aggregation-induced emission, mechanochromism and blue electroluminescence of carbazole and triphenylamine-substituted ethenes. J Mater Chem C 2014;2:4320–7.
[43] Odom SA, Lancaster K, Beverina L, Lefler KM, Thompson NJ, Coropceanu V, et al. Bis [bis-(4-alkoxyphenyl) amino] derivatives of dithienylethene, bithiophene, dithienothiophene and dithienopyrrole: palladium-catalysed synthesis and highly delocalised radical cations. Chem Eur J 2007;13:9637–46.
[44] Krejčík M, Daněk M. Hart1 F. Simple construction of an infrared optically transparent thin-layer electrochemical cell: applications to the redox reactions of ferrocene, $Mn_2(CO)_{10}$ and $Mn(CO)_3$(3,5-di-t-butyl-catecholate)−. J Electroanal Chem Interfacial Electrochem 1991;317:179–87.
[45] Sheldrick GM. SHELXS-97, a program for crystal structure solution. Göttingen, Germany: University of Göttingen; 1997.
[46] Sheldrick GM. SHELXL-97, a program for crystal structure refinement. Göttingen, Germany: University of Göttingen; 1997.
[47] Frisch MJ, Trucks GW, Schlegel HB, Scuseria GE, Robb MA, Cheeseman JR, et al. Gaussian 09, revision D.01. Wallingford CT: Gaussian, Inc.; 2009.
[48] Cossi M, Rega N, Scalmani G, Barone V. Energies, structures, and electronic properties of molecules in solution with the C-PCM solvation model. J Comput Chem 2003;24:669–81.
[49] Barone V, Cossi M. Quantum calculation of molecular energies and energy gradients in solution by a conductor solvent model. J Phys Chem A 1995-2001;1998:102.
[50] Chen Z, Li Z, Hu F, Yu GA, Yin J, Liu SH. Novel carbazole-based aggregation-induced emission-active gold(I) complexes with various mechanofluorochromic behaviors. Dyes Pigments 2016;125:169–78.
[51] Luo X, Zhao W, Shi J, Li C, Liu Z, Bo Z, et al. Reversible switching emissions of tetraphenylethene derivatives among multiple colors with solvent vapor, mechanical, and thermal stimuli. J Phys Chem C 2012;116:21967–72.
[52] Chen Z, Liang J, Nie Y, Xu X, Yu GA, Yin J, et al. A novel carbazole-based gold(I) complex with interesting solid-state, multistimuli-responsive characteristics. Dalton Trans 2015;44:17473–7.
[53] Chen Z, Yang L, Hu Y, Wu D, Yin J, Yu GA, et al. Carbazole-based gold(I) complexes with alkyl chains of different lengths: tunable solid-state fluorescence, aggregation-induced emission (AIE), and reversible mechanochromism characteristics. RSC Adv 2015;5:93757–64.
[54] Li H, Chi Z, Xu B, Zhang X, Li X, Liu S, et al. Aggregation-induced emission enhancement compounds containing triphenylamine-anthrylenevinylene and tetraphenylethene moieties. J Mater Chem 2011;21:3760–7.
[55] Kazmaier PM, Hoffmann R. A theoretical study of crystallochromy quantum interference effects in the spectra of perylene pigments. J Am Chem Soc 1994;116:9684–91.
[56] Ou YP, Zhang J, Zhang F, Kuang D, Hartl F, Rao L, et al. Notable differences between oxidized diruthenium complexes bridged by four isomeric diethynyl benzodithiophene ligand. Dalton Trans 2016;45:6503–16.
[57] Zhang J, Ou Y, Xu M, Sun C, Yin J, Yu GA, et al. Synthesis and characterization of dibenzoheterocycle-bridged dinuclear ruthenium alkynyl and vinyl complexes. Eur J Inorg Chem 2014:2941–51.
[58] Robson KCD, Sporinova B, Koivisto BD, Schott E, Brown DG, Berlinguette CP. Systematic modulation of a bichromic cyclometalated ruthenium (II) scaffold bearing a redox-active triphenylamine constituent. Inorg Chem 2011;50:6019–28.
[59] Polit W, Mücke P, Wuttke E, Exner T, Winter RF. Charge and spin confinement to the amine site in 3-connected triarylamine vinyl ruthenium conjugates. Organometallics 2013;32:5461–72.